Article

Observation of the elevation of cholinesterases activity in brain glioma by a near-infrared emission chemsensor

Yanyan Ma, Wenjie Gao, Shihan Ma, Yongyuan Liu, and Weiying Lin

Anal. Chem., **Just Accepted Manuscript** • DOI: 10.1021/acs.analchem.0c02770 • Publication Date (Web): 31 Aug 2020

Observation of the elevation of cholinesterases activity in brain glioma by a near-infrared emission chemsensor

Yanyan Ma, Wenjie Gao, Shihan Ma, Yongyuan Liu, and Weiying Lin*

Institute of Fluorescent Probes for Biological Imaging, School of Chemistry and Chemical Engineering, School of Materials Science and Engineering, University of Jinan, Jinan, Shandong 250022, P.R. China

* E-mail: weiyinglin2013@163.com

ABSTRACT: The excessive expression of cholinesterases (ChEs) directly disturbs the metabolism of acetylcholine (ACh), causing disordering neurotransmission in the brain or even Alzheimer's disease and cancer. However, the variation of ChEs including cetylcholinesterase and butyrylcholinesterase in brain glioma has not yet been investigated. Therefore, the development of a suitable method for in situ imaging ChEs in brain tissue to understand the physiological functions of ChEs in depth is very important. Herein, a new near-infrared emission fluorescent probe (**IPAN**) for visualization of ChEs activity was developed. **IPAN** exihibits ultrafast response to ChEs, low detection limit for AChE (0.127 U/mL) and BChE (0.0117 U/mL) as well as a large Stokes shift with near-infrared emission. Based on these excellent attributes, the **IPAN** was effectively utilized for imaging the fluctuations of ChEs activity in the apoptosis cells and zebrafish. Notably, by utilizing the unique probe **IPAN**, we observed a significant enhancement of ChEs activity in the tumor cells and brain glioma, for the first time. We believe that this interesting finding could provide a powerful guidance for tumor resection in the future.

Acetylcholine (ACh), the important neurotransmitter in the central nervous system, was significantly associated to recognition, learning, emotion and behavior. [1-3] It is reported that the decrease of ACh in brain could cause neurotransmitter metabolism dysfunction and several diseases. [4-6] Cholinesterases (ChEs), which contains two major forms acetylcholinesterase (AChE) and butyrylcholinesterase (BChE), could hydrolyze ACh to choline and acetic acid in cholinergic synapses. [7,8] The excessive expression of ChEs directly disturbs the metabolism of ACh, thus disordering neurotransmission in the brain and even lead to depressive disorders, Alzheimer's disease and Parkinson's disease. [9-11] Furthermore, the anomalous expression of ChEs may promote cell proliferation and participate in tumorigenesis.[12,13] However, the molecular mechanisms of ChEs in cancer, especially in the complex brain, is still unclear. Therefore, the development of a suitable method for in situ imaging ChEs in brain tumor to understanding the physiological functions of ChEs in depth is very highly significant.

Currently, several methods have been used for the detection of ChEs, including choline oxidase coupled multi-enzyme assay, Ellman's colorimetric method and electrochemical analysis. [14-16] However, these methods have several shortcomings, such as laboring pretreatment, time-consuming procedures and unsuitable for living biological systems detection. Fluorescence imaging, as a potential approach, has attracted significant attention owing to their inherent advantages including excellent compatibility, high spatiotemporal resolution and real-time in-situ observation. [17-19] Very recently, some fluorescent probes for the detection of ChEs activity have been reported. [20-25] However, additional excellent attributes of the probes for detection of ChEs are still needed to be improved to study the internal relationship between ChEs and diseases in vivo. For instance, large Stokes shifts with near infrared emission, which could achieve deep tissue penetration and avoid self-absorption of fluorescence, [26,27] fast response for ChEs, which could detect the fluctuation of ChEs rapidly in situ. Notably, to the best of our knowledge, the detection of ChEs activity in the brain glioma has not been reported yet. Therefore, the construction of a near infrared emission fluorescent probe with large Stoke shift for fast observation of the activity of ChEs in the brain tumour is urgently required.

Herein, we have developed a new near-infrared emission fluorescent probe (**IPAN**) for detection of ChEs activity. The new probe **IPAN** demonstrated ultrafast response to ChEs with a large Stokes shift, excellent photo-stability and selectivity. **IPAN** was successfully utilized for visualization the changes of ChEs activity in the apoptosis cells and zebrafish which induced by H_2O_2. Significantly, an obvious enhancement of ChEs activity in the brain glioma was revealed by **IPAN** for the first time.

Experimental Section

Synthesis of the probe IPAN

Compound **IPAH** (149 mg, 0.5 mmol) and cesium carbonate (163 mg, 0.5 mmol) were added to dichloromethane, and the mixture was stirred for 30 min under N_2 atmosphere at room temperature. Then, 100 μL dimethylcarbamoyl chloride

was added to the above stirred mixture. Additional dimethylcarbamoyl chloride needed to be added every 12 h. After 72 h, the mixture was purified by column chromatography (petroleum ether : CH_2Cl_2:MeOH=10:30:1) to afford a yellow product (yield 80%). ^{1}H NMR (400 MHz, DMSO) δ 7.72 (d, J = 8.4 Hz, 3H), 7.34 (dd, J_1 = 37.4 Hz, J_2 = 16.2 Hz, 2H), 7.16 (d, J = 8.8 Hz, 2H), 6.89 (s, 1H), 3.04 (s, 3H), 2.92 (s, 3H), 2.62 (s, 2H), 2.55 (s, 2H), 1.02 (s, 6H). ^{13} C (101 MHz, DMSO) δ 170.82, 156.32, 154.18, 152.69, 137.17, 133.44, 129.78, 129.25, 123.20, 122.78, 114.32, 113.49, 76.78, 42.79, 38.64, 36.78, 36.60, 34.36, 32.14, 27.90. HRMS (ESI): calcd. for $C_{22}H_{23}N_3O_2$, $[M+H]^+$, m/z, 362.1863, found: 362.1863.

Cell imaging experiments

Before the imaging experiments, the NHA and U87 cells were incubated into confocal plates for 24 h. Then the cells were treated with 10 μM **IPAN** respectively for 30 min and washed twice with PBS. The fluorescence images were acquired with Nikon A1R confocal microscope.

For the imaging of apoptotic cells, the NHA cells were pretreated with 1 mM H_2O_2 for 1 h. After that the NHA cells were further incubated with 10 μM **IPAN** for another 30 min and prepared for imaging. Emission was collected at 663-738 nm (excited at 561 nm) for red channel. The mean fluorescence intensity of each cell was measured (via "Measure" function) and averaged across the three fields imaged.

Zebrafish imaging experiments

3-day-old zebrafish were purchased from the Nanjing EzeRinka Biotechnology Co., Ltd.. Zebrafish were transferred into confocal plates, and cultured in 1 mM H_2O_2 for 30 min. Then the zebrafish were transferred to fresh water containing 10 μM **IPAN** for another 30 min. After that, the zebrafish were anesthetized and imaged. The statistical analysis was performed from three separate biological replicates. The excitation wavelength was 561 nm and the emission wavelength was collected at 663-738 nm.

Mouse brain slices fluorescence imaging

The 4-week old nude mice and nude mice were purchased from Shandong University. All of the animal experiments were carried out according to the Animal Management Rules of the Ministry of Health in People's Republic of China (Document NO. 55, 2001) and the guidelines for the Care and Use of Animal Ethical Experimentation Committee of Shandong University.

For the brain glioma imaging. U87 cells were injected into nude mice by subcutaneously manner for the growth of xenografts tumor. After about 14 days, the glioma and brain were excised from nude mice and cut into about 500 μm slices. The slices were cultured with 20 μM **IPAN** for 30 min and imaged.

Results and Discussion

Molecular design and synthesis

The probe of **IPAN** was designed by introducing an N, N-dimenthyl carbamyl moiety into **IPAH** through the acylation reaction (Scheme S1). We speculated that the probe itself was no fluorescence due to quenched group of carbamyl in the **IPAN**. After addition of ChEs, the dimethyl carbamate moiety was recognized, the ester bond was cleaved and then **IPAN** was transformed to **IPAH** (Scheme 1). The characterizations of **IPAN** were provided in the Supporting Information.

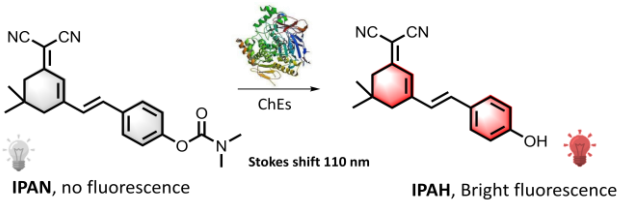

Scheme 1. Sensing mechanism of the probe **IPAN** for the detection of ChEs.

Optical properties of the probe IPAN for ChEs

We evaluated the optical properties of **IPAN** toward ChEs initially. The absorption of the free probe **IPAN** was approximately centered at 570 nm. In the presence of AChE or BChE, a marked enhancement at this absorption peak can be observed (Figure S1). The fluorescence titrimetric spectra were then examined under the excitation at 545 nm. As shown in Figure 1A and B, **IPAN** emitted a faint emission band at 654 nm (quantum yield, φ=0.038). Addition of increasing concentration of AChE or BChE resulted in obvious fluorescence increases gradually, indicating that **IPAN** was transformed to **IPAH**. Obviously, the **IPAN** possessed a large Stokes' shift which could avoid self-absorption of fluorescence. The probe **IPAN** could determine AChE or BChE activity in the range 0−80 U/mL or 25-31 U/mL with a linear relationship (Figure 1C and D). The detection limit of **IPAN** for AChE or BChE were calculated as 0.127 U/mL or 0.0117 U/mL. Moreover, the fluorescence quantum yield of **IPAN** was obviously increased after treated with AChE (φ=0.12) or BChE (φ=0.19). In addition, the probe could detect AChE or BChE activity quickly in less than 3s (Figure 2A and Figure S2) and its fluorescence intensity remained stable within 1 h (Figure S3), suggesting that the probe **IPAN** have a potential for real-time detection the enzyme activity in living system. The sensing mechanism of **IPAN** toward AChE or BChE was characterized by HRMS analysis. As shown in Figure S4, in the presence of AChE or BChE, the probe displayed a main peak at m/z 291.1484 or 291.1580, which is consistent with **IPAH** (calcd 291.1492 for $C_{19}H_{18}N_2O$), demonstrating that the reaction mechanism is similar as the depicted in Scheme 1. All these data show that **IPAN** can detect AChE and BChE activity.

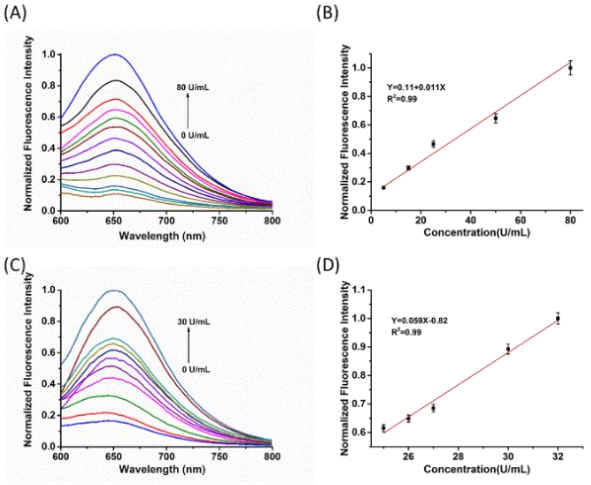

Figure 1. (A) The fluorescence spectra of **IPAN** in the presence or absence of various concentration of AChE (0-80 U/mL) (B) The linear relationship between the normalized fluorescence intensity at 654 nm and the concentration of AChE. (C) Fluorescence titration spectra of **IPAN** for sensing different concentration of BChE (0-30 U/mL). (D) The linear relationship between normalized fluorescence intensity at 654 nm with 21 U/mL-31 U/mL BChE.

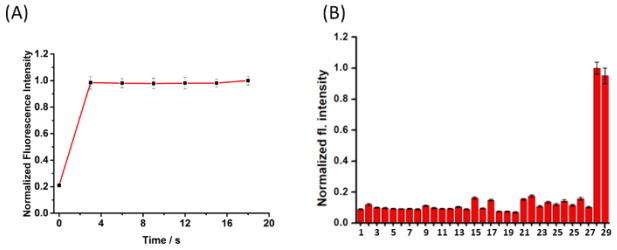

Figure 2. (A) Time-dependent fluorescence intensity of **IPAN** (10 μM) for response AChE activity. (B) Fluorescence responses of **IPAN** (10 μM) to various representative analytes in PBS (pH 7.4, 20 mM, 50% DMSO) buffer: **IPAN** (10 μM), $CaCl_2$ (1 mM), $CuCl_2$ (1 mM), DTBP (500 μM), GSH (2.5 mM), Hcy (1 mM), Cys (1 mM), KCl (1 mM), KNO_3 (1 mM), Na_2S (1 mM), NaBr (1 mM), KF (1 mM), Na_2HPO_4 (1 mM), NH_4OAc (1 mM), $ZnCl_2$ (1 mM), CH_3CHO (500 μM), $MgCl_2$ (1 mM), $FeSO_4$ (1 mM), H_2O_2 (500 μM), NaClO (500 μM), BSA (10 μg/mL), HSA (10 μg/mL), DMEM, alkaline phosphatase (50 U/mL), phospholipase (50 U/mL), chymotrypsin (50 U/mL), thrombin (50 U/mL), lysozyme (50 U/mL), trypsin (50 U/mL), AChE (80 U/mL) and BChE (27 U/mL). λ_{ex} = 545 nm.

Fluorescence imaging of ChEs activity in living cells

The feasibility of **IPAN** for imaging ChEs activity in living cells was then investigated. Before imaging, the cytotoxicity of **IPAN** was firstly evaluated by MTT assay. As shown in Figure S6, NHA and U87 cells treated with different concentrations of **IPAN** (0-50 μM) displayed high cell viability above 90%, suggesting that the probe possessed low toxicity for living cells and was suitable for living organisms imaging.

We next moved on our attention to explore the ability of **IPAN** for imaging the changes of ChEs in living cells. Previous studies reported that H_2O_2 could induce cells apoptosis which is related to the change of ChEs activity. [28,29] Therefore, we aimed to use the probe **IPAN** to detect ChEs activity in living cells during apoptosis induced by H_2O_2. As shown in Figure 3, the NHA cells cultured with 1 mM H_2O_2 for 1h displayed stronger fluorescence signals than the untreated cells. In order to further confirm the changes of fluorescence intensity was caused by the increase of ChEs activity, NHA cells were treated with donepezil, the inhibitor of ChEs. [30] As expected, the fluorescent intensity of these cells was weak, indicating that the enhancement of fluorescence signal is ascribed to the over-activity of ChEs upon apoptosis and the probe can be used for detection the changes of ChEs in living cells.

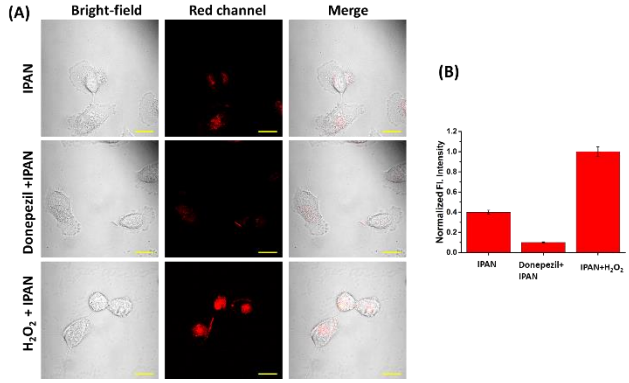

Figure 3. (A) Fluorescence imaging of ChEs in living cells. First row (**IPAN**): NHA cells incubated with 10 μM **IPAN**. Second row (Donepezil + **IPAN**): NHA cells were pre-treated with 10 μM donepezil for 1 h and then stained with 10 μM **IPAN**. Third row (H_2O_2 + **IPAN**): NHA cells were pre-cultured with 1 mM H_2O_2 for 1 h and then incubated with 10 μM **IPAN**. (B) Fluorescence quantitative analysis of A. Red channel: λ_{ex} = 561 nm, λ_{em} = 663−738 nm. Scale bar: 20 μm.

It is reported that the activity of ChEs is accompanied with brain tumor. [31,32] Therefore, we selected U87 (human glioma) cells as research object to investigate how ChEs activity varied by using **IPAN**. As expected, the NHA cells cultured with **IPAN** for 30 min exhibited weak fluorescence (Figure 4). However, when U87 cells stained with **IPAN**, a brighter emission was obtained. To verify that the increase of fluorescence signal was came from ChEs activity, an inhibitor of ChEs, donepezil, incubated with NHA cells for 1 h. The cells treated with donepezil for 1 h exhibited lower emission than cells without donepezil, indicating that the activity of ChEs was increased in U87 cells. These data displayed that the activity of ChEs was enhanced in living glioma cells.

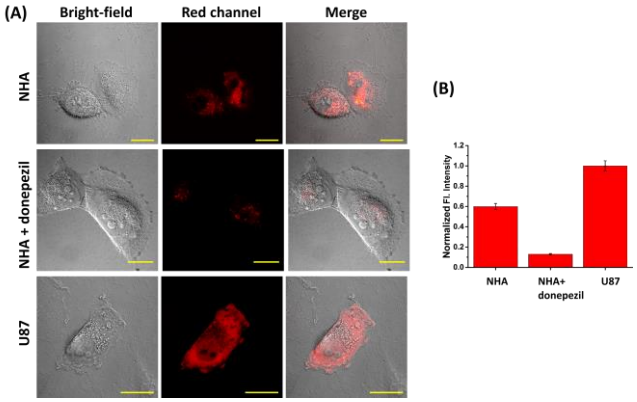

Figure 4. (A) Fluorescence images of living cells. First row (NHA): NHA cells were cultured with **IPAN** for 30 min. Second row (NHA +donepezil): NHA cells pre-treated with donepezil for

1 h and then stained with **IPAN** for 30 min. Third row (U87): U87 cells incubated with **IPAN** for 30 min. (B) Fluorescence quantitative analysis of A. Red channel: λ_{ex} = 561 nm, λ_{em} = 663−738 nm. Scale bar: 20 μm.

Fluorescence imaging of ChEs activity in living zebrafish

Inspired by the successful application of **IPAN** in cellular imaging, we intended to further explore the performance of **IPAN** for detection of ChEs activity in living small-animal. Zebrafish were used as living organism model due to their genes are similar to human beings. [33,34] As shown in Figure 5, when the zebrafish stained with only probe **IPAN** for 30 min, a dark fluorescence signal in the red channel was detected. By contrast, the zebrafish pre-incubated with H_2O_2 for 1 h, a significant enhancement of fluorescence signal was observed, suggesting that the probe **IPAN** is capable of imaging the changes of ChEs activity in living zebrafish.

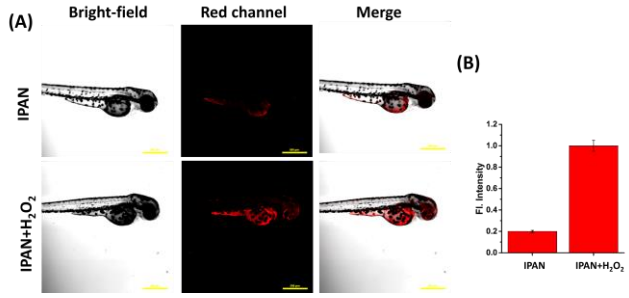

Figure 5. (A) Fluorescence imaging of ChEs activity in zebrafish First row (**IPAN**): zebrafish were incubated with 10 μM **IPAN** for 30 min. Second row (**IPAN** + H_2O_2): Zebrafish were pre-treated with 1 mM H_2O_2 for 1 h and then stained with 10 μM **IPAN** for 30 min. (B) Fluorescence quantitative analysis of A. Red channel: λ_{ex} = 561 nm, λ_{em} = 663−738 nm. Scale bar: 20 μm.

Fluorescence imaging of ChEs activity in living glioma

Motivated by the excellent attributes of **IPAN** for distinguishing cancer form normal cells, we further attempted to verify the suitable of **IPAN** for imaging the changes of ChEs in brain tumor and normal brain. The nude mice were pre-inoculated U87 cells before 14 days for imaging, then the brain of normal mice and glioma tissue of tumour mice were excised and cut into 500 μM for imaging. As presented in Figure 6, the normal brain exhibited a dark emission intensity, however, the fluorescence intensity of glioma tissue enhanced about 2-fold than the normal brain tissue, indicating that the activity of ChEs was elevated in brain tumor. Importantly, it is the first time that the enhancement activity of ChEs in brain glioma tissue was monitored by using a unique fluorescence probe. In addition, the activity of ChEs in whole blood of living tumor-loaded mice and living normal mice were determined. The whole blood were obtained from normal and tumor-bore living mice respectively, then diluted 500-fold with PBS buffer and measured finally with fluorescence spectrometer. The blood of the tumor mice indicated a distinct fluorescence elevation (about 2-fold) than that of the blood of normal mice (Figure S7). All of these data show that the probe was successfully detected the fluctuation of ChEs activity in tumor mice and normal mice for the first time.

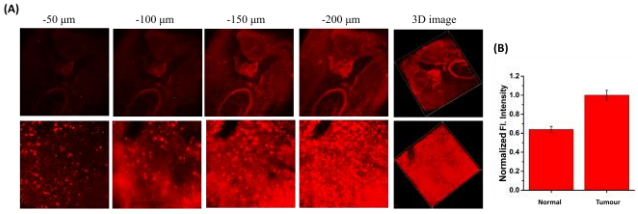

Figure 6. (A) Fluorescence images normal brain (first row) and brain glioma by using the probe **IPAN** for 30 min incubation. (B) Fluorescence quantitative analysis of A.

Conclusion

In summary, we have presented a new near-infrared emission fluorescence probe for real time imaging ChEs activity *in vitro* and *in vivo*, particularly in brain glioma for the first time. The powerful probe **IPAN** possesses ultrafast response, high sensitivity, low detection limit and large Stokes shift. Based on these excellent attributes, the **IPAN** was successfully used to detect the changes of ChEs activity in the living cells and zebrafish during apoptosis. Notably, the in situ imaging studies by the probe **IPAN** revealed, for the first time, that the activity of ChEs in the tumor cells and brain glioma was higher than that of the normal cells and brain. We believe that this novel NIR probe could serve as a powerful tool for exploring the roles of ChEs activity in biological and pathological processes and provide a guide for further diagnosis and treatment of ChEs related diseases.

ASSOCIATED CONTENT

Supporting Information

The Supporting Information is available free of charge on the ACS Publications website. Synthesis of the probes, absorption and fluorescence spectra, imaging assays, ^{1}H NMR and ^{13}C NMR spectra. (PDF)

AUTHOR INFORMATION

Corresponding Author

*Fax: + 86-531-82769031. E-mail: weiyinglin2013@163.com.

Notes

The authors declare no competing financial interest.

ACKNOWLEDGMENT

This work was financially supported by NSFC (21472067, 21672083, 21877048), Taishan Scholar Foundation (TS201511041), and the startup fund of University of Jinan (309-10004).

REFERENCES

(1) Baig, A. M.; Rana, Z.; Tariq, S.; Lalani, S.; Ahmad, H., Traced on the timeline: discovery of acetylcholine and the components of the human cholinergic system in a primitive unicellular eukaryote acanthamoeba spp. *ACS Chem. Neurosci.* **2017,** *9*, 494-504.

(2) Wang, C.-I.; Periasamy, A. P.; Chang, H.-T., Photoluminescent C-dots@RGO probe for sensitive and selective detection of acetylcholine. *Anal. Chem.* **2013,** *85*, 3263-3270.

(3) Miyakawa, T.; Yamada, M.; Duttaroy, A.; Wess, J., Hyperactivity and intact hippocampus-dependent learning in mice lacking the M1 muscarinic acetylcholine receptor. *J. Neurosci.* **2001,** *21*, 5239-5250.

(4) Anagnostaras, S. G.; Murphy, G. G.; Hamilton, S. E.; Mitchell, S. L.; Rahnama, N. P.; Nathanson, N. M.; Silva, A. J., Selective cognitive dysfunction in acetylcholine M_1 muscarinic receptor mutant mice. *Nat. Neurosci.* **2003,** *6*, 51-58.

(5) Muir, J. L., Acetylcholine, aging, and Alzheimer's disease. *Pharma. Biochem. Be.* **1997,** *56*, 687-696.

(6) Mitchell, K. M., Acetylcholine and choline amperometric enzyme sensors characterized in vitro and in vivo. *Anal. Chem.* **2004,** *76*, 1098-1106.

(7) Miao, Y.; He, N.; Zhu, J.-J., History and new developments of assays for cholinesterase activity and inhibition. *Chem. Rev.* **2010,** *110*, 5216-5234.

(8) Mikalsen, A.; Andersen, R. A.; Alexander, J., Use of ethopropazine and BW 284C51 as selective inhibitors for cholinesterases from various species. *Comp. Biochem. Physiol. C: Comp. Pharmacol.* **1986,** *83*, 447-449.

(9) Soreq, H.; Seidman, S., Acetylcholinesterase-new roles for an old actor. *Nat. Rev. Neurosci.* **2001,** *2*, 294-302.

(10) Mineur, Y. S.; Obayemi, A.; Wigestrand, M. B.; Fote, G. M.; Calarco, C. A.; Li, A. M.; Picciotto, M. R., Cholinergic signaling in the hippocampus regulates social stress resilience and anxiety-and depression-like behavior. *Proc. Natl. Acad. Sci.* **2013,** *110*, 3573-3578.

(11) Lane, R. M.; Potkin, S. G.; Enz, A., Targeting acetylcholinesterase and butyrylcholinesterase in dementia. *Int. J. Neuropsychopharmacol.* **2006,** *9*, 101-124.

(12) Soreq, H.; Lapidot-Lifson, Y.; Zakut, H., A role for cholinesterases in tumorigenesis? *Cancer Cells*. **1991**, *3*, 511-516.

(13) Razon, N.; Soreq, H.; Roth, E.; Bartal, A.; Silman, I., Characterization of activities and forms of cholinesterases in human primary brain tumors. *Exp. Neurol.* **1984**, *3*, 681-695.

(14) Gill, R.; Bahshi, L.; Freeman, R.; Willner, I., Optical detection of glucose and acetylcholine esterase inhibitors by H_2O_2-sensitive CdSe/ZnS quantum dots. *Angew. Chem. Int. Edit.* **2008,** *47*, 1676-1679.

(15) Solna, R.; Dock, E.; Christenson, A.; Winther-Nielsen, M.; Carlsson, C.; Emnéus, J.; Ruzgas, T.; Skládal, P., Amperometric screen-printed biosensor arrays with co-immobilised oxidoreductases and cholinesterases. *Anal. Chim. Acta* **2005,** *528*, 9-19.

(16) Fenoy, G. E.; Marmisollé, W. A.; Azzaroni, O.; Knoll, W., Acetylcholine biosensor based on the electrochemical functionalization of graphene field-effect transistors. *Biosens. Bioelectron.* **2020,** *148*, 111796-111799.

(17) Lakowicz, J. R., *Principles of fluorescence spectroscopy*. Springer, New York, 3rd edn, 2006.

(18) Spangler, B.; Morgan, C. W.; Fontaine, S. D.; Vander Wal, M. N.; Chang, C. J.; Wells, J. A.; Renslo, A. R., A reactivity-based probe of the intracellular labile ferrous iron pool. *Nat. Chem. Biol.* **2016,** *12*, 680-685.

(19) Cao, D.; Liu, Z.; Verwilst, P.; Koo, S.; Jangjili, P.; Kim, J. S.; Lin, W., Coumarin-based small-molecule fluorescent chemosensors. *Chem. Rev.* **2019,** *119*, 10403-10519.

(20) Deng, W.; Chen, P.; Hu, P.; He, Z.; Zhang, M.; Yuan, X.; Huang, K., Enzymatic reaction modulated synthesis of quantum dots for visual detection of cholinesterase activity and inhibitor. *Sens. Actuators, B* **2019,** *292*, 180–186.

(21) Xu, X.; Cen, Y.; Xu, G.; Wei, F.; Shi, M.; Hu, Q., A ratiometric fluorescence probe based on carbon dots for discriminative and highly sensitive detection of acetylcholinesterase and butyrylcholinesterase in human whole blood. *Biosens. Bioelectron.* **2019,** *131*, 232-236.

(22) Liu, S.; Xiong, H.; Yang, J.; Yang, S.; Li, Y.; Yang, W.; Yang, G., Discovery of butyrylcholinesterase-activated near-infrared fluorogenic probe for live-cell and in vivo imaging. *ACS Sens.* **2018**, *3*, 2118-2128.

(23) Ma, J.; Si, T.; Yan, C.; Li, Y.; Li, Q.; Lu, X.; Guo, Y., Near-infrared fluorescence probe for evaluating acetylcholinesterase (AChE) activity in PC12 cells and in situ tracing ache distribution in zebrafish. *ACS Sens.* **2020**, *5*, 83-92.

(24) Yoo, S.; Han, M., A fluorescent probe for butyrylcholinesterase activity in human serum based on a fluorophore with specific binding affinity for human serum albumin. *Chem. Commun.* **2019**, *55*, 14574-14577.

(25) Wang, X.; Li, P.; Ding, Q.; Wu, C.; Zhang, W.; Tang B., Observation of acetylcholinesterase in stress-induced depression phenotypes by two-photon fluorescence imaging in the mouse brain. *J. Am. Chem. Soc.* **2019**, *141*, 2061−2068.

(26 Chen, H.; Dong, B.; Tang, Y.; Lin, W., A unique "integration" strategy for the rational design of optically tunable near-infrared fluorophores. *Acc. Chem. Res.* **2017,** *50*, 1410-1422.

(27 Sednev, M. V.; Belov, V. N.; Hell, S. W., Fluorescent dyes with large Stokes shifts for super-resolution optical microscopy of biological objects: a review. *Methods Appl. Fluoresc.* **2015,** *3*, 042004.

(28 Antunes, F.; Cadenas, E.; Brunk, U. T., Apoptosis induced by exposure to a low steady-state concentration of H_2O_2 is a consequence of lysosomal rupture. *Biochem. J.* **2001,** *356*, 549-555.

(29 Yang, L.; He, H.-Y.; Zhang, X.-J., Increased expression of intranuclear AChE involved in apoptosis of SK-N-SH cells. *Neurosci. res.* **2002,** *42*, 261-268.

(30) Kosasa, T.; Kuriya, Y.; Matsui, K.; Yamanishi, Y., Inhibitory effect of orally administered donepezil hydrochloride (E2020), a novel treatment for Alzheimer's disease, on cholinesterase activity in rats. *Eur. J. Pharmacol.* **2000,** *389*, 173-179.

(31) Razon, N.; Soreq, H.; Roth, E.; Bartal, A.; Silman, I., Characterization of activities and forms of cholinesterases in human primary brain tumors. *Exp. Neurol.* **1984,** *84*, 681-695.

(32) Vidal, C. J., Expression of cholinesterases in brain and non-brain tumours. *Chem. Biol. Interact.* **2005,** *157*, 227-232.

(33) Lieschke, G. J.; Currie, P. D., Animal models of human disease: zebrafish swim into view. *Nat. Rev. Genet.* **2007,** *8*, 353-367.

(34) Amatruda, J. F.; Patton, E. E., Genetic models of cancer in zebrafish. *Int. Rev. Cell Mol. Biol.* **2008,** *271*, 1-34.

For TOC only

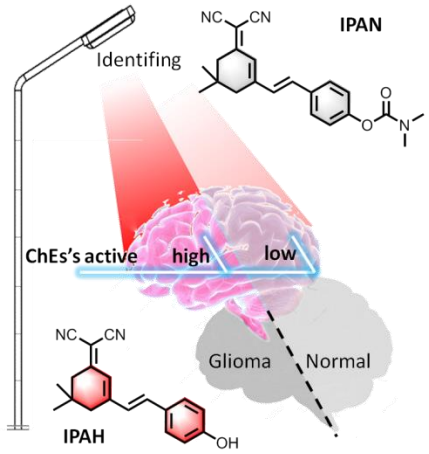
Identifing
IPAN
NC
CN
O
O
N
ChEs's active
high
low
Glioma
Normal
IPAH
OH